THE ASTRONOMICAL JOURNAL VOLUME 103, NUMBER 3 MARCH 1992

A PROPER MOTION SURVEY. I. HYADES AND UMa MOVING GROUPS

RENÉ MÉNDEZ,[1] M. T. RUIZ, J. MAZA, AND M. WISCHNJEWSKY
Departamento de Astronomía, Universidad de Chile, Casilla 36-D, Santiago, Chile
Received 24 September 1990; revised 13 August 1991

ABSTRACT

We analyze the results of a proper motion survey in a couple of ESO *R* 5°×5° fields, finding evidence for faint (and primarily red) members of the Hyades and UMa moving groups. By using the velocity ellipsoid of the Hyades and UMa streams and the technique described by Méndez & Ruiz [AJ, 103, 911 (1992)] we estimate number densities and nonbiased velocity dispersions for each moving group. Our results suggest that the Hyades moving group extends at least 96 pc in the solid angle covered by our survey, while the UMa moving group shows a decrease in density past 36 pc, indicating that we are looking beyond it. The large tangential velocity dispersion for both moving groups suggest on the other hand that they are not gravitationally bound.

1. INTRODUCTION

Since Proctor found, in 1869, that several stars in a wide field around the Hyades cluster showed similar proper motions, and the subsequent discovery by Hertzsprung, in 1909, that the same is true for Ursa Major cluster, there has been some discussion about the existence of large-scale moving clusters on which the Sun is immersed.

Delhaye (1948) and Eggen (1958, 1959) arrived at the conclusion that there are many more stars (spread all over the sky) with a spatial motion similar to that of the Hyades or UMa streams than the predicted numbers drawn from a random sample.

Ogorodnikov & Latyshev (1968, 1970) showed that the probability of having an observed concentration of convergent points from a Poisson distribution (i.e., by chance) similar to the observed one is smaller than 10^{-6} for both Hyades and UMa moving groups, therefore also supporting the existence of these large-scale clusters. Eggen (1984, 1985, 1986) has investigated the bright stars in the solar vicinity to increase the statistics of members associated to the Hyades or UMa moving groups.

However, the existence of these moving clusters is still not widely accepted mainly because the hypothesis of an ellipsoidal velocity distribution implies that a nonzero fraction of the field stars have the same spatial motions than those of the Hyades or UMa moving clusters. This brings as consequence that the actual number of stars associated to each of the moving clusters remains unknown.

In what follows we present the results of a proper motion survey on the Hyades and UMa moving groups in ESO areas 439 and 440 which analyzes the tangential kinematics of much fainter objects than those analyzed by the previous authors. We show that there exists evidence for both moving groups in our sample and that by using the formalism presented by Méndez & Ruiz (1992, hereafter referred to as MR), it is possible to estimate number densities and nonbiased velocity dispersions for the members of each moving group.

A catalogue containing our proper motions for this and other ESO fields that are being measured will be published elsewhere. That catalogue will also contain spectrophotometric information that is being currently analyzed for selected objects in our survey.

[1] Present address: Yale University, Astronomy Department, P.O. Box 6666, New Haven, CT 06511.

2. THE DATA

Positions were determined using a semiautomatic *x-y* measuring machine (brand Ascorecord 3030 build by Zeiss, Jena) on those high proper motion objects previously identified using an eye stereo comparison (blink) machine (also build by Zeiss, Jena). The surveyed two-epoch plates were glass copies of the ESO R Survey: IIIaF beyond an RG630 filter, with an exposure time of 2 hr and a plate limit of around 21 mag, taken with the ESO Schmidt telescope (for area ESO 440 a new original second-epoch plate was obtained). The plate scale is 67.5″/mm and the field of view is 5°×5°.

Reference objects on the same magnitude range of the program stars (around 18th magnitude) and distributed uniformly all over the plates were selected among those objects which did not show an appreciable proper motion in the stereo comparison machine. For the setup of the blink machine, it should be possible to detect displacements down to about 7 μm or 0.5″ as it was found to be the case (see discussion on completeness in Sec. 3), although this limit is obviously magnitude dependent. It takes about 50 hr to scan a pair of plates, where every single image is carefully checked for proper motion. To measure positions, each 30×30 cm^2 plate was divided in nine subzones of square shape so that it was possible to measure both program and reference stars during the same continuous 3–4 hr session in each subzone. In every 10×10 cm^2 subzone we selected 25 reference stars.

Although the precision of the measuring machine fluctuates between 1.1 and 1.6 μm in each coordinate, with a mean of 1.3 μm, there are recognized systematic effects that can deteriorate the accuracy up to about 3 μm (Kinner 1976; Méndez 1989).

The (x,y) coordinates for the reference stars on each subzone (for a given epoch) were mapped on the corresponding subzone for the next/previous epoch separately, using a bilinear model that proved to be good given the small field (around 1.7°×1.7°) covered by each of the subzones. The coefficients of that model were calculated, as usual, using a least squares fit and rejecting reference objects whose residual proper motion was higher than 3 times the current value of the standard deviation in the corresponding coordinate, as calculated from the model. That procedure was ended when the model's standard deviation was less than or equal to 1.8 μm in each coordinate, which corresponds to the mean expected error in the difference of positions due to the precision of the measuring machine. In ESO 439 we used an aver-

 0004-6256/92/030904-07$00.90

age of 18.8 reference stars per subzone, while this number was higher in ESO 440 (see below). Using the model described above, proper motions μ_x and μ_y were evaluated separately on each subzone. Given that there are very few standard reference stars (around 17 per subzone if we use the SAO Catalogue) and that their magnitude distribution is so different from that of our program stars, we decided to work directly on μ_x and μ_y proper motions instead of transforming them to $\mu_\alpha \cos\delta$ and μ_δ using a catalogue of positions and proper motions. Since it is expected that the x coordinate is lined up with the α coordinate and the y coordinate with the δ coordinate, we will suppose that this is the case approximating $\mu_\alpha \cos\delta$ by μ_x and μ_δ by μ_y (see Sec. 4).

The surveyed zones where ESO area 439 and ESO area 440. These adjacent zones were selected so that the angular distance between its centers and the convergent points of the Hyades and UMa moving groups, as given by Eggen (1984), is about 90°, and, therefore, the tangential velocity for those objects associated to them is expected to be maximum. The coordinates (B1950.0) for the area centers are ($11^h 30^m2 - 30°09'$) for ESO 439 and ($11^h 53^m4, -30°08'$) for ESO 440.

We identified 250 and 493 high proper motion stars in ESO 439 and ESO 440, respectively. The change in the number of objects is due exclusively to the different time base in both cases: 6.9 yr for ESO 439, and 9.0 yr for ESO 440 (both areas are at about 30° to the north of the Galactic plane). Visual estimates suggest that most of our proper motion selected stars have magnitudes in the range $10 \leqslant m_R \leqslant 21$. We do not have photometry for all of our stars and we have not imposed magnitude limits *a posteriori* on our sample, we are only restricted by the limiting magnitude of the ESO plates.

The mean error on the total proper motions, as derived from the discrepancy on the proper motion of objects located in the overlapping border of two subzones, is 0.048″/yr for ESO 439 and 0.026″/yr for ESO 440. The difference in errors is due in part to the different time base and in part due to a slightly different procedure used to link reference stars on a given subzone and epoch to the same subzone in the next-/previous epoch. In ESO 440 we used, besides the 25 reference stars per subzone that we used in ESO 439, five additional stars per adjacent border and one per each vertex. Therefore, the central subzone has 49 reference stars while a border subzone has only 36. The purpose of this procedure was to provide enough reference stars in the borders of each subzone to avoid extrapolation of the calibrated mapping of one set of reference stars (on a given epoch) on the same set for the next/previous epoch. It should be noted that the above quoted errors are upper limits because they were evaluated at the borders of each subzone where the bilinear model is perhaps not as good as in the middle of the subzone due to large-scale distortions that are known to be present in the Schmidt plates (see, e.g., Peñaloza 1981) and which were already minimized by dividing the plate in several subzones.

Given that the mean uncertainty σ_μ does not change with μ in the range considered here, the percentual error on μ increases as the proper motion decreases in absolute value. In order to limit that percentual error we decided to work with those proper motion stars in which the mean error on μ does not exceed 50%. That means we should trim our data at 0.096″/yr on ESO 430 and at 0.052″/yr on ESO 440. A compromise value between those two values is 0.06″/yr in which case the maximum percentual error for both samples combined is 56%, were we weighted by the number of objects in each area. There are 223 objects in ESO 439 that satisfies $\mu \geqslant 0.06$″/yr, while this number is 406 for ESO 440.

With the data trimmed as above outlined and taking into account the uncertainties on each coordinate, the mean error in the position angle (P.A.) for the 629 stars is 13.4°, although this value decreases up to 10.6° if we cut the sample at $\mu = 0.1$″/yr (see Sec. 3). Therefore there is no ambiguity if we define a 10° bin for the observed P.A. histograms.

The P.A. histograms for each area are shown in Figs. 1 and 2. It is quite obvious that the distribution is not random and that there are preferred directions of motion. The observed structure cannot be explained exclusively as a reflex of the Sun's peculiar motion whose apex is at P.A. 65° so that the field stars show a relative, fictitious, motion to the P.A. 245° which coincides with one of the observed maxima. The lateral maxima (P.A. $\theta \simeq 140°$ and other less obvious at P.A. $\theta \simeq 280°$) correspond to the projected motion of the objects associated to the UMa and Hyades moving groups, respectively, as we will show in what follows using the formalism presented by MR.

3. COMPARISON WITH THEORY

In order to compare the observed P.A. histogram with that obtained from a velocity ellipsoid theory, we should generate some parameters for both, Hyades and UMa moving clusters, as described by MR. These parameters correspond to the projection of the velocity ellipsoid on the center of the field considered and are defined by the tangential velocity centroids $V_{\alpha 0}$ and $V_{\delta 0}$ (which determine the position of the peak in P.A. of the distribution), the velocity dispersion σ_α and σ_δ in each tangential coordinate (which determine the width in P.A. of the distribution), and the correlation coefficient r (which determine the asymmetry of the P.A. distribution). Each of these parameters depend on the director cosines of the area center considered, therefore we should generate a set of them for each of the two fields, ESO 439 and ESO 440. However, given that the number of objects in each 10° bin is relatively small and in order to avoid small

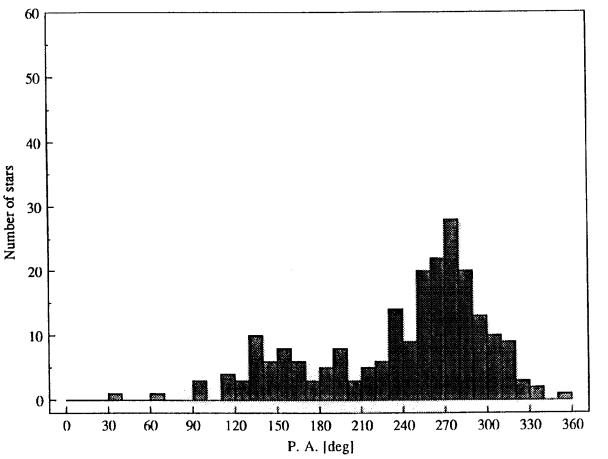

FIG. 1. Position angle histogram for those objects with $\mu \geqslant 0.06$″/yr in the field of ESO 439. The bin width is 10°.

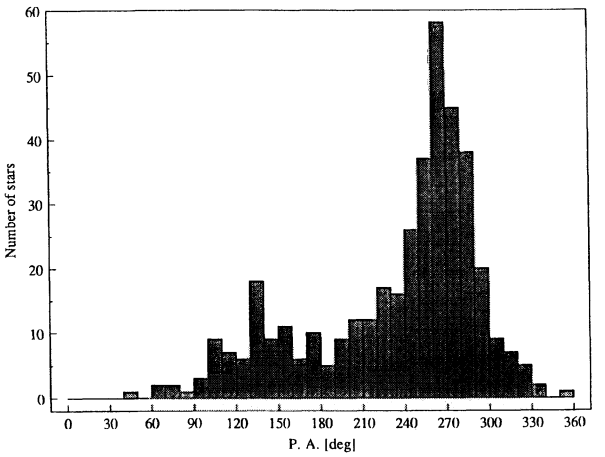

FIG. 2. Same as Fig. 1 but for ESO 440.

number fluctuations we combined the proper motions from both plates (see Fig. 3). Evidently this procedure is only valid when the variation from field to field of the velocity ellipsoid centroid is smaller than the errors associated to the positioning of the maxima in the histograms, as it is the case here where the two fields are next to each other. In this case it has more sense to use as center of the field the weighted mean of the coordinates for each plate. That center turns out to be (11^h45^m1, $-30°08'$). Using Eqs. (26) and (27) and Table I of MR and the previous coordinates, we evaluated the needed velocity ellipsoid parameters. They are shown in Table 1.

In order to compare the observed histogram (Fig. 3) with the expected P.A. distribution $\Gamma_\theta(\theta)$ as given by MR, it is necessary to integrate that distribution on the width of the bin, 10°, obtaining an expected histogram. That expected histogram, using the values of Table 1, is shown in Fig. 4. It is clear that the observed and expected maxima coincide, although the formal (velocity) dispersions for both moving groups are smaller than that of our sample, as expected (see MR). Notice that in Fig. 4, the reflex solar motion distribution has been normalized to the total number of objects in our sample with $\mu \geqslant 0.06''$/yr (629 stars).

TABLE 1. Velocity ellipsoid parameters for our field centroid.

Parameter	Hyades	UMa	Reflex basic solar motion
$V_{\alpha 0}$ km/s	− 44.65	10.68	− 13.96
$V_{\delta 0}$ km/s	8.17	− 14.19	− 5.42
σ_α km/s	0.73	0.65	20.00
σ_δ km/s	1.91	0.67	20.00
r	0.15	0.94	0.00

To estimate the meaningful number densities and velocity dispersions for each moving group in the solid angle covered by our survey, we need to know the proper motion completeness limit of our sample. To do that we will start by assuming that our sample is not proper motion limited in which case the joint expected P.A. histogram produced by the reflex solar motion and both moving groups is given by Eqs. (19), (20), and (21) of MR that we reproduce here in the abbreviated form as

$$\Gamma_{\rm tot}(\theta) = N_{\rm UMa}\Gamma_\theta^{\rm UMa}(\theta) + N_{\rm Hyades}\Gamma_\theta^{\rm Hyades}(\theta) + N_f\Gamma_\theta^f(\theta), \quad (1)$$

where $N_{\rm UMa}$, $N_{\rm Hyades}$, and N_f are the number of stars associated to the UMa, Hyades and field, respectively. In Fig. 5 we present the best χ^2 fit of Eq. (1) to the observed histogram.

With the (approximate) fit of Fig. 5 we can isolate the less contaminated regions (in P.A) to extract possible members following the kinematics of each moving group and the field. Now, as it was shown in MR, the log of the cumulative proper motion distribution follows a straight line as a function of $\log \mu$. Deviation of the exponent -3 in such a relation could signal the onset of incompleteness provided that the spatial distribution of the analyzed objects is homogeneous. A set of spatially homogeneous objects can be found in our sample

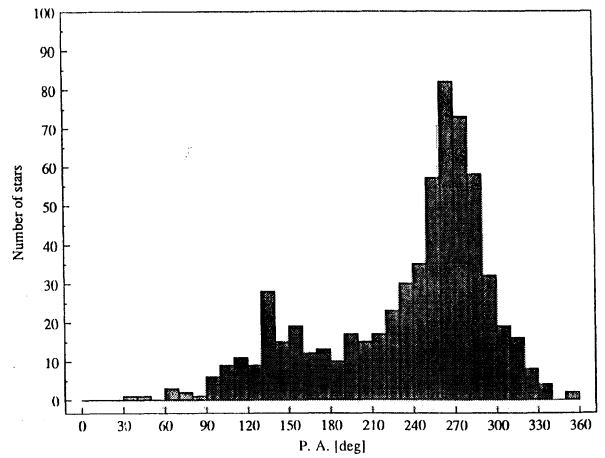

FIG. 3. Resulting position angle after combining those objects with $\mu \geqslant 0.06''$/yr in the field of ESO 439 and ESO 440. The bin width is 10°.

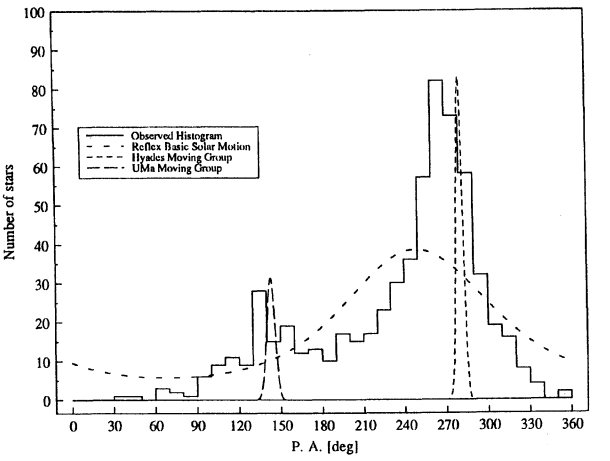

FIG. 4. Expected position angle histogram superimposed on the histogram of Fig. 3. The reflex solar motion histogram has been normalized to the number of stars in the observed histogram.

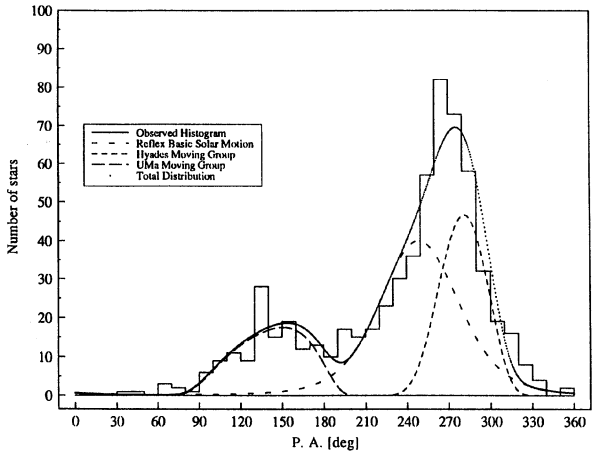

FIG. 5. The best χ^2 fit of the expected position angle histogram to the observed one by using Eq. (1) of the text.

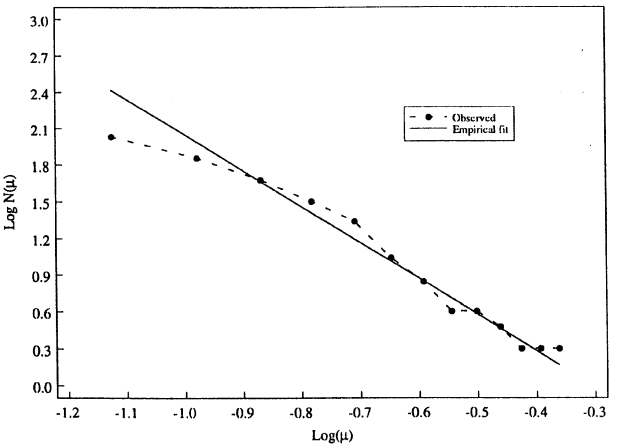

FIG. 7. Logarithm of the cumulative proper motion histogram for the field objects of Fig. 6. The points here corresponds to the points in Fig. 6 and they are joined by a broken line. The continuous line is the empirical fit down to 0.1″/yr given by Eq. (2) of the text.

ments are a reflex of the solar motion and whose spatial distribution can be considered isotropic in the solar vicinity. We selected such objects from those which have proper motions with P.A. in the range $195° \leqslant \theta \leqslant 245°$ (see Fig. 5) where it is expected that the contamination by UMa and Hyades objects is small.

The resulting μ distribution for field objects is shown in Fig. 6. The cumulative distribution satisfies the relationship

$$\log\left(\frac{N(\mu)}{f}\right) = (-2.95 \pm 0.16)\log\mu + (-0.898 \pm 0.09), \quad (2)$$

only down to $\mu_l \simeq 0.1''/\text{yr}$ (Fig. 7), value which we will consider the completeness limit of our sample [in Eq. (2), f is a correction factor greater than one, due to the fact that we extracted only a subsample of the field objects]. The above completeness limit is consistent with the expected 0.5″ minimum displacement for detection in the blink machine (see Sec. 2).

With a completeness limit of $\mu_l = 0.1''/\text{yr}$ we will be able to detect UMa members up to a distance of about 38 pc, and up to about 96 pc for Hyades members (to compute the above distances we have used our Table 1, and Eq. (14) of MR]. If any one of these two moving groups has a size (in the observed direction) smaller than the size mentioned above, we should observe a depression in the μ distribution of objects associated to that moving group. The μ distribution for the less contaminated samples of both moving groups are shown in Figs. 8 and 9, where the Hyades members were extracted from the P.A. range $270° \leqslant \theta \leqslant 300°$, while the UMa members were extracted from the P.A. range $120° \leqslant \theta \leqslant 160°$ (see Fig. 5).

The Hyades distribution (Fig. 8) shows a behavior similar to that of the field objects, indicating that its size is at least 96 pc in this direction. However due to the high degree of contamination by field objects, a distortion of the intrinsic structure is expected. The situation is more favorable and interesting for the UMa distribution. Figure 9 shows that there exist a sharp decrease in the number of stars for $\mu \leqslant 0.105''/\text{yr}$.

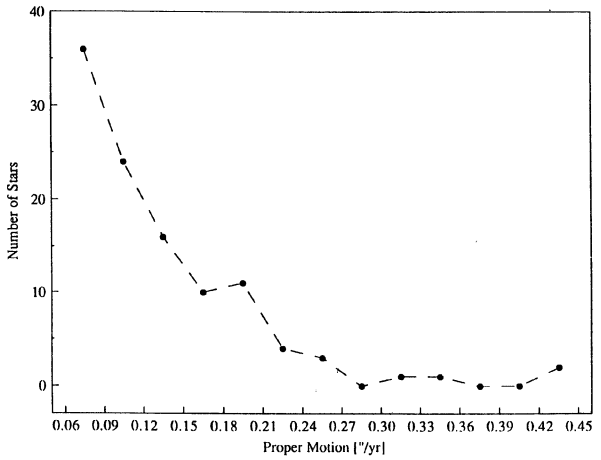

FIG. 6. Proper motion histogram of a subsample of field objects. The bin width is 0.03″/yr.

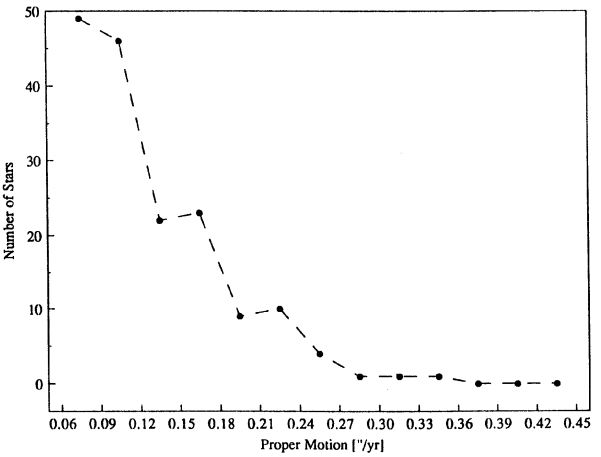

FIG. 8. Proper motion histogram of a subsample of Hyades moving group members. The bin width is 0.03″/yr.

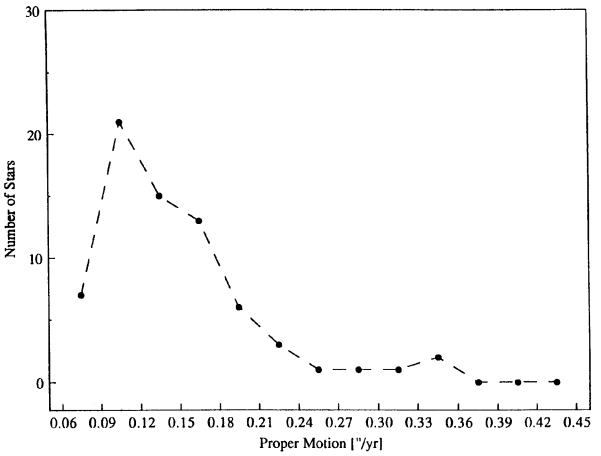

FIG. 9. Same as Fig. 8 but for UMa moving group members.

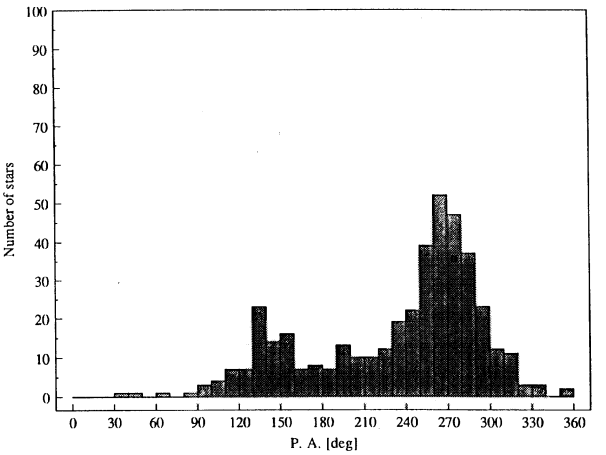

FIG. 11. Position angle histogram for ESO 439 and ESO 440 combined with $\mu \geqslant 0.1''$/yr. The bin width is 10°.

Even though the quoted value is slightly over the completeness limit, the observed structure is not present in the distribution for the field objects (see normalized histogram in Fig. 10), suggesting that it is not a problem of incompleteness but rather a real decrease in the number density of stars associated to that group for distances $\geqslant 36$ pc. If that is true, we are looking beyond the moving group and, therefore, our counts include essentially all the objects associated to the UMa group in this direction of the sky. This last statement is not true for Hyades, where we only have an inferior limit for the number of objects associated to it.

In light of the above discussion we restricted even further our sample, selecting only those objects with $\mu \geqslant 0.1''$/yr. In doing so we discard a fair number of objects and the sample is even poorer and, therefore, more sensitive to small number statistics, but we win by knowing the spatial extent in which the sample is complete, allowing the evaluation of number densities. Also the percentual error in the position angles and proper motions is obviously smaller. The P.A. histogram for the 415 objects with $\mu \geqslant 0.1''$/yr is shown in Fig. 11.

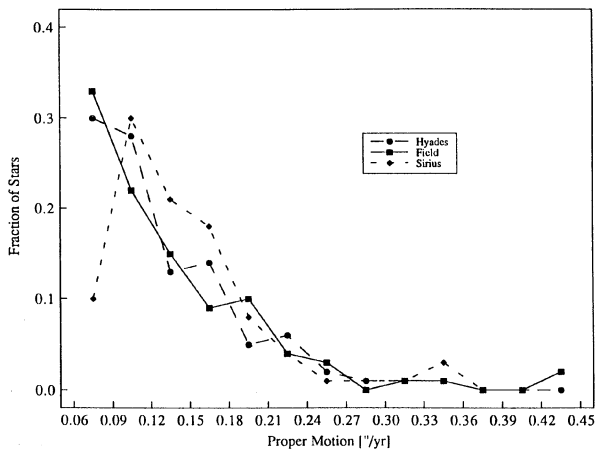

FIG. 10. Normalized proper motion histogram for Hyades, Field, and UMa. Note the sharp decline in the counts of UMa members for $\mu \leqslant 0.105''$/yr.

In our approximate fit of Fig. 5 we have assumed that proper motion selection effects are small. However, in Fig. 11 we have explicitly cut our sample at the completeness limit, so that our assumptions need to be revised accordingly. For that matter, we have used the approach suggested in MR; Eqs. (24) and (25). Those equations assume that we know the proper motion completeness limit of the sample and that the parallax distribution is homogeneous (along the line of sight, but no necessarily across the sky). Therefore, to apply such an approach, we have to make sure that both moving groups are indeed uniformly distributed (we have already shown that that is the case for the field, see the above discussion on completeness limit). It turns out that, above $\mu = 0.1''$/yr, the proper motion distribution of UMa stars follows approximately that of a uniform distribution. The Hyades stars show an apparent departure of 25% from a uniform distribution [the slope in the $\log N(\mu)$ vs $\log \mu$ relationship is -4] although this could well be a consequence of contamination from field objects as discussed previously. Therefore the data does not preclude to assume a uniform parallax distribution.

Now, if we assume a uniform parallax distribution for the field objects and for both moving groups, the joint expected P.A. histogram is given by [See Eq. (25) in MR]

$$\Gamma_{\rm tot}(\theta) = \Gamma_{\theta}^{\rm UMa}(\theta) + \Gamma_{\theta}^{\rm Hyades}(\theta) + \Gamma_{\theta}^{f}(\theta), \qquad (3)$$

where the P.A. distribution functions are given by Eq. (24) in MR.

Our best χ^2 fit using the above approach is shown in Fig. 12, while the derived parameters from the fit are shown in Table 2.

Errors in the proper motions (or for this matter in the P.A.) have a minor impact in our results as shown in Fig. 13 where we present the χ^2 fit of Fig. 12 and its convolution with an error function represented by a Gaussian with a FWHM of 21.2° (corresponding to the observed P.A. error, Sec. 2).

4. COMPARISON WITH OTHER RESULTS

Ogorodnikov & Lathyshev (1968, 1970) estimated an inferior limit of 10^5 and 2×10^3 stars associated to the Hyades and UMa moving groups, respectively, in the Sun's vicinity

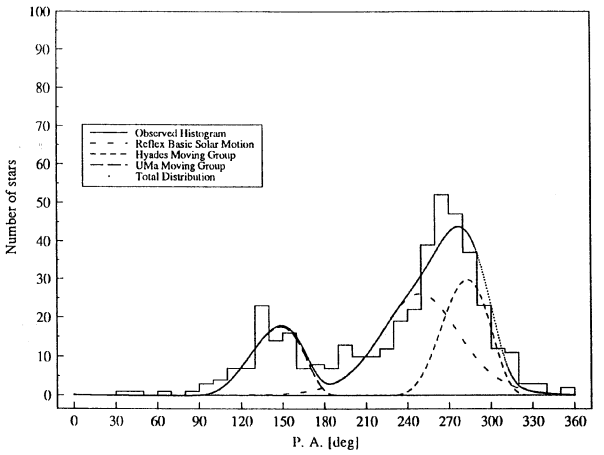

FIG. 12. The best χ^2 fit of the expected position angle histogram [Eq. (3) of the text] to the observed histogram. The sample is complete in μ. The derived parameters are shown in Table 2.

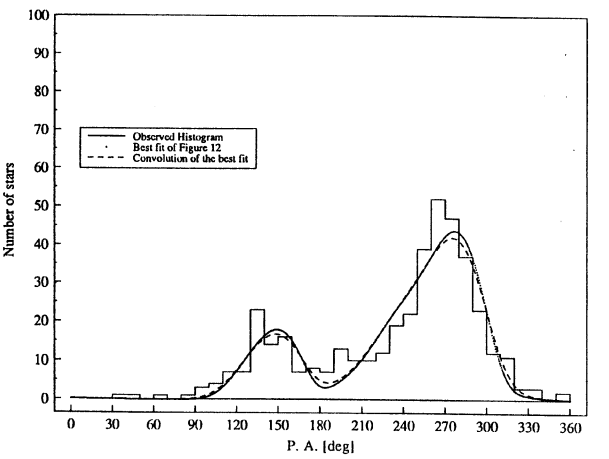

FIG. 13. Convolution of the total histogram of Fig. 12 with a Gaussian of FWHM of 21.2°. Effects on our derived parameters due to errors in P.A. are negligible.

($d \leqslant 20$ pc). If we extend our results of Table 2 to the same volume of sky we find that there are about 10^3 stars associated to the Hyades moving group and about 9×10^3 stars associated to UMa. From the counts of objects associated to each moving cluster Ogorodnikov and Lathyshev found that $N_{\text{Hyades}}/N_{\text{UMa}} \simeq 2$, ratio which in our case is 1.5. We should mention that the estimates done by the previous authors are mainly qualitative and therefore could be subjected to large uncertainties.

Ogorodnikov & Lathyshev (1968) also evaluated number densities for each moving group, obtaining $n_{\text{Hyades}} \simeq 0.0040$ stars/pc^3 and $n_{\text{UMa}} \simeq 0.0025$ stars/pc^3. The densities we found are much higher (Table 2). Here we should mention that the previous authors made the approximation $n_{\text{Hyades}}/n_{\text{Field}} \simeq N_{\text{Hyades}}/N_{\text{Field}}$ and the same for UMa, using $n_{\text{Field}} \simeq 0.12$ stars/pc^3. Therefore they assumed that the surveyed volume for the field and moving group members is the same, something that in the case of proper motion surveys is not true as we already discussed.

We were surprised by the number densities of the UMa moving group and the field, since those values are much larger than the currently accepted density of 0.12 stars/pc^3 for the entire solar vicinity (see, e.g., Lang 1980). This finding could have several explanations.

(1) The luminosity function at the faint end of the UMa moving cluster is more populated than previously thought. Recently, Gilmore *et al.* (1989) have shown that any local missing mass has to be distributed with a scale height of $\leqslant 60$ pc above the galactic plane. Therefore an important question would be to estimate the faint end contribution to the global star (and mass) density of the solar neighborhood from this suspected moving group.

(2) The star density in the solar neighborhood is highly inhomogeneous with strong variations across the sky, having a mean value of 0.12 stars/pc^3.

(3) The moving group theory is not appropriate to describe the kinematic of those nearby stars represented in our sample. More specifically, some of the fixed parameters used to construct the P.A. distribution [e.g., velocity centroids ($V_{\alpha 0}, V_{\delta 0}$), etc.] which have been taken from the literature are not appropriate to our sample.

To decide which of the above alternatives is the correct one we should wait for the results in other selected areas on which measurements and analysis are underway. With a larger database, involving different regions of the sky, it will be possible to decide if alternative 2 is viable. Also it will be very interesting to test if general models for the kinematics of stars in the solar neighborhood provide a better fit to the observed distributions in proper motion and position angle. Such models exist (e.g., Ratnatunga *et al.* 1989) and have proved to be very successful in predicting several kinematics observables. By comparing the results of those general models and the moving group theory it may be possible to decide about the statistical significance of introducing extra components represented by the long advocated Eggen's moving groups. It is indeed interesting to notice that our best fits fail to predict a couple of features in the P.A. histogram: The sharp peak at about P.A. = 265° (see the excess stars in the observed distribution, Fig. 12), and the valley between 170° and 200° where there is again an excess of stars over the predicted number from our best fit models.

A thorough comparison between the moving group idea and the above-mentioned models should however wait until new areas are measured and more data (particularly photometry) is obtained to better define the selection effects on our sample. We are also in the process of analyzing spectroscopic data on selected objects of our sample to see if the assumptions mentioned in point 3 above are appropriate, mainly if the astrometric distances [Eq. (14) of MR] are in accordance with the derived spectroscopic distances.

In relation to the velocity dispersions, Johnson & Soderblom (1987) found a value of 3.8 km/s for the UMa group

TABLE 2. Number densities and velocity dispersions for each moving group and the field.

Moving group	Number density stars/pc^3	Velocity dispersion km/s
Hydes	0.024	13.2
UMA	0.260	5.3
Reflex basic Solar motion	0.360	14.4

from Eggen's (1983) data and of 6.6 km/s using Palouš & Hauck's (1986) data. That last value is comparable to our result of 5.3 km/s (tangential component). For the Hyades moving group, the formal velocity dispersion given by Eggen (1984) is 1.5 km/s, which is an inferior limit for the physical dispersion as discussed in MR.

Luyten (1965) has made a (photographic) blue proper motion survey with a 48″ Schmidt telescope (the scale plate was 5.2″/mm). He surveyed a center at (11^h42^m, $-24°$) (B1950.0) which we analyzed with the techniques described above. Using the velocity dispersion as given in Table 2, we found that there is, again, a very good correlation between the observed and expected P.A. histograms. This result also gives us confidence in the goodness (in statistical terms) of the approximation $\mu_x \simeq \mu_\alpha \cos\delta$ and $\mu_y \simeq \mu_\delta$ (see Sec. 2).

5. CONCLUSIONS

It was shown that the observed P.A. histograms can be fitted by the expected histograms from a velocity ellipsoid theory whose parameters were constructed from a totally independent data base in relation to our sample. This constitutes an evidence in favor of the existence of large-scale moving groups containing those bright early type stars studied by Eggen as well as the faint red stars of our sample.

The large nonbiased velocity dispersion estimated for both clusters suggests, however, that they are far from being gravitationally bound and that they are, therefore, in a process of dilution. It would be very interesting to have the necessary observations for the objects associated to both moving groups in order to set their masses and to evaluate mass densities from the number densities presented here and thus decide if the density is smaller than the critical density for a gravitationally bound system. It will also be interesting to know the radial kinematics of these objects to confirm their association to the moving groups and to estimate radial velocity dispersions.

We would like to thank Dr. R. West for kindly sending us glass copies of the ESO *R* plates, Dr. H. Schuster for taking new epoch plates with the Schmidt Camera at La Silla, M. Takamiya for her help in making some of the graphs, and to an anonymous referee for his/her valuable suggestions. This work was part of a Master's Thesis at the Astronomy Department of the University of Chile. This research received support from Grant Fondecyt 0989/89. R. M. acknowledges also a thesis fellowship from Grant Fondecyt 0989/89.

REFERENCES

Delhaye, J. 1948, Bull. Astron. Inst. Neth. 10, 409
Eggen, O. J. 1958, MNRAS, 118, 65
Eggen, O. J. 1959, Obs, 79, 143
Eggen, O. J. 1983, AJ, 88, 642
Eggen, O. J. 1984, AJ, 89, 1350
Eggen, O. J. 1985, PASP, 97, 807
Eggen, O. J. 1986, PASP, 98, 423
Gilmore, G., Wyse, R. F. G., & Kuijken, K. 1989, ARA&A, 27, 555
Hertzsprung, E. 1909, ApJ, 30, 135
Johnson, D. R. H., & Soderblom, D. R. 1987, AJ, 93, 864
Kinner, M. 1976, Jena Rev., 3, 151
Lang, K. R. 1980, Astrophysical Formulae, 2nd ed. (Springer, Berlin)
Luyten, W. J. 1965, Proper Motions Survey with the Forty-Eight Inch Schmidt Telescope. VI. Four Southern Regions (University of Minnesota Press, Minnesota)
Méndez, R. 1989, M. Sc. thesis, University of Chile
Méndez, R., & Ruiz, M. T. 1992, AJ, 103, 911
Ogorodnikov, K. F., & Latyshev, I. N. 1968, SvA, 12, 279
Ogorodnikov, K. F., & Latyshev, I. N. 1970, SvA, 13, 934
Palouš, J., & Hauck, B. 1986, A&A, 162, 54
Peñaloza, M. A. 1981, RMxA&A, 6, 129
Proctor, R. A. 1869, Proc. R. Soc. London, 18, 169
Ratnatunga, K. U., Bahcall, J. N., & Casertano, S. 1989, ApJ, 339, 106